



Selective Augmentation of Stem Cell Populations in Structural Fat Grafts for Maxillofacial Surgery

Luigi Clauser¹*, Letizia Ferroni²*, Chiara Gardin², Riccardo Tieghi¹, Manlio Galiè¹, Giovanni Elia¹, Adriano Piattelli³, Paolo Pinton⁴, Eriberto Bressan⁵, Barbara Zavan^{2*}

1 Unit of Cranio Maxillo Facial Surgery, Center for Craniofacial Deformities and Orbital Surgery – Reference Center for Rare Disease, Sant'Anna Hospital and University, Cona, Ferrara, Italy, **2** Department of Biomedical Sciences, University of Padova, Padova, Italy, **3** Department of Medical, Oral, and Biotechnological Sciences, University of Chieti-Pescara, Chieti, Italy, **4** Department of Morphology, Surgery and Experimental Medicine, Section of Pathology Oncology and Experimental Biology, University of Ferrara, Ferrara, Italy, **5** Department of Neurosciences, University of Padova, Padova, Italy

Abstract

Structural fat grafting utilizes the centrifugation of liposuction aspirates to create a graded density of adipose tissue. This study was performed to qualitatively investigate the effects of centrifugation on stem cells present in adipose tissue. Liposuction aspirates were obtained from healthy donors and either not centrifuged or centrifuged at 1,800 rpm for 3 minutes. The obtained fat volumes were divided into three layers and then analyzed. The results demonstrate that centrifugation induces a different distribution of stem cells in the three layers. The high-density layer displays the highest expression of mesenchymal stem cell and endothelial markers. The low-density layer exhibits an enrichment of multipotent stem cells. We conclude that appropriate centrifugation concentrates stem cells. This finding may influence the clinical practice of liposuction aspirate centrifugation and enhance graft uptake.

Citation: Clauser L, Ferroni L, Gardin C, Tieghi R, Galiè M, et al. (2014) Selective Augmentation of Stem Cell Populations in Structural Fat Grafts for Maxillofacial Surgery. PLoS ONE 9(11): e110796. doi:10.1371/journal.pone.0110796

Editor: Gwendolen Reilly, University of Sheffield, United Kingdom

Received: June 29, 2014; **Accepted:** September 1, 2014; **Published:** November 6, 2014

Copyright: © 2014 Clauser et al. This is an open-access article distributed under the terms of the Creative Commons Attribution License, which permits unrestricted use, distribution, and reproduction in any medium, provided the original author and source are credited.

Data Availability: The authors confirm that all data underlying the findings are fully available without restriction. All relevant data are within the paper and its Supporting Information files.

Funding: The work was supported by Progetto di Ateneo University of Padova, Italy. The funder had no role in study design, data collection and analysis, decision to publish, or preparation of the manuscript.

Competing Interests: The authors have declared that no competing interests exist.

* Email: barbara.zavan@unipd.it

† These authors contributed equally to this work.

Introduction

Over the past two decades, the treatment of soft tissue loss with structural fat grafting (SFG) has yielded encouraging clinical results in terms of the texture, softness, and quality of skin patterns [1–3]. Autologous fat tissue transfer is thought to provide an ideal filler for soft tissue augmentation because fat tissue is biocompatible, versatile, natural looking, readily available, abundant, and inexpensive and because fat tissue can be harvested easily and repeatedly with minimal trauma to the donor sites. Implanted fat has the potential to be permanent; however, this fat can be removed if required [4–6]. Fat grafting has become increasingly popular because of the ability to remove fat from sites of excess fat and then implant the fat into sites of fat deficiency, allowing the body to be sculpted. This procedure was proposed by Coleman and was first applied for facial remodeling and for breast reconstruction and augmentation [7–10]. This procedure is typically considered safe and involves autologous tissue injection at a defective site directly after harvesting without ex vivo expansion [11–15]. However, fat grafting is not without disadvantages. Infection and damage to local nerves, muscles, glands, and blood vessels during harvest are always possible [7,16–18]. Several studies have also reported disappointing short-term survival rates for implanted fat or excessive growth of transplanted fat. Irregular reabsorption remains a problem when using

autologous, non-vascularized free-fat grafts to correct soft tissue defects [19–23]. Growth factors, beta-blockers, insulin, growth media, and hyperbaric oxygen have been used to prevent irregular resorption [24]. Although satisfactory results can be achieved during the early postoperative period, long-term results may be disappointing for both the patient and surgeon [25–27]. The most common difficulty is the estimated reabsorption rate. In light of such considerations, despite the widespread clinical use of SFG, little is known regarding the cell quality (the most important factor in fat grafting) when the tissue is injected into the patient. Therefore, the aim of the present study was to analyze the stemness properties of cells within fat that was aspirated and centrifuged according to Coleman's technique. Specifically, we performed molecular and cellular analyses of the stemness properties of cells distributed in the fat following the centrifugation required by Coleman's procedure.

Materials and Methods

Ethics statement

The Ethical Committee of Ferrara Hospital, Ferrera, Italy approved the research protocol. Written informed consent was obtained from all patients, in accordance with the Helsinki Declaration, before their inclusion in this study.

Coleman's procedure

Using Coleman's procedure, fat was collected at the Cranio Maxillo Facial Surgery Unit at St. Anna Hospital, Ferrara, Italy and at the University of Ferrara, Ferrara, Italy from 30 healthy patients (age: 21–36 years old; BMI: 30–38; 25 females, 5 males) under general anesthesia; the patients were undergoing cosmetic surgery procedures. The fat donor sites were the abdominal area, love handles, inner sides of the thigh and knees, and flanks. The fat was collected using a cannula (Byron Medical (a division of Mentor Corporation), Tucson, AZ, USA) connected to a 10 ml Luer-Lok syringe (BD Syringe Luer-Lok tip; Becton Dickinson, Franklin Lakes, NJ, USA). The samples were sealed and centrifuged at 1800 rpm (rotor size: 16 cm; g force: 580) for 3 min. After centrifugation, the samples were separated into three layers: an upper yellow layer of oil derived from destroyed fat fragments, a middle layer composed of the adipose tissue graft, and a bottom layer of blood. The upper layer was discarded by ejection after rotating the syringe. Codman neuropads (Codman Neuro Sciences, Sarl, Switzerland) were used to wick the residual oil component. The lower layer was discarded by opening the plug from the Luer-Lok connection. The middle layer of fat was divided into three parts:

- the first 3 ml is referred to as the low-density layer (LDL),
- the central 3 ml is the middle-density layer (MDL), and
- the final 3 ml is the high-density layer (HDL), which is in the lower part of the syringe near the needle (obtained after the removal of red cells).

DNA content

The DNA content was determined using a DNeasy kit (Qiagen, Hilden, Germany) to isolate the total DNA from cell cultures following the manufacturer's protocol for tissue isolation and an overnight incubation period with proteinase K (Qiagen). The DNA concentration was determined by measuring the absorbance at 260 nm using a spectrophotometer. Then, the cell number was determined using a standard curve (micrograms of DNA vs. cell number) generated by DNA extraction from counted cells. The standard curve was linear over the tested range of 5–80 μg DNA ($r = 0.99$).

Real-time PCR

Total RNA was extracted using an RNeasy Lipid Tissue kit (Qiagen), including DNase digestion with the RNase-Free DNase Set (Qiagen), from the adipose tissue of the three different layers of the centrifuged lipoaspirate and from non-centrifuged lipoaspirate samples. In total, 800 ng of RNA was reverse-transcribed using an RT² First Strand kit (Qiagen). Real-time PCR was performed according to the user's manual for the Human Mesenchymal Stem Cell RT2 Profiler PCR Array (SABiosciences, Frederick, MD, USA) and using RT² SYBR Green ROX FAST Master Mix (Qiagen). Thermal cycling and fluorescence detection were performed using a Rotor-Gene Q 100 (Qiagen). The data were analyzed using Excel-based PCR Array Data Analysis Templates (SABiosciences). The results are reported as ratios with respect to the mRNA expression levels of non-centrifuged fat.

Oil red O (ORO) staining

LDL-, MDL-, and HDL-derived cells were fixed in 4% formalin and stained with 0.3% ORO (Sigma-Aldrich, St. Louis, MO, USA) in 60% isopropanol. After washing with 60% isopropanol, the cells were acquired, and the dye was extracted with 100% isopropanol. The optical density (OD) of each solution was

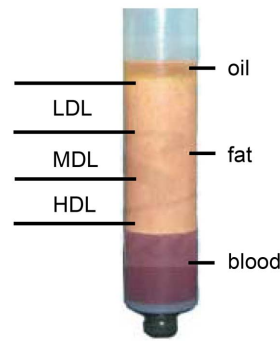


Figure 1. Coleman's procedure. After centrifugation for 3 min at 1800 rpm, the fat sample is separated into three layers: an upper yellow layer of oil, a middle layer of adipose tissue, and a bottom layer of blood. The top and bottom layers are discarded. The middle layer is divided into three distinct layers: a low-density layer (LDL), a middle-density layer (MDL), and a high-density layer (HDL).
doi:10.1371/journal.pone.0110796.g001

measured at 520 nm using a Victor 3 spectrophotometer (Perkin Elmer, Waltham, MA, USA).

Immunocytochemical staining

The cells were layered and fixed on coverslips and then incubated in 2% bovine serum albumin (BSA, Sigma-Aldrich) solution in phosphate-buffered saline (PBS) for 30 minutes at room temperature. Then, the sections were incubated with the primary antibodies in 2% BSA solution in a humidified chamber overnight at 4°C. The following primary antibodies were used: rabbit polyclonal anti-human osteonectin antibody (1:1000, AB1858, Millipore Corporation, MA, USA), chicken polyclonal anti-human Tubulin $\beta 3$ antibody (1:1000, AB9354, Millipore Corporation), rabbit polyclonal anti-human GFAP antibody (1:100, AB5804, Millipore Corporation), rabbit polyclonal anti-human von Willibrand Factor antibody (1:100, A0082, Dako, Milan, Italy), mouse monoclonal anti-human CD31 antibody (10 $\mu\text{g}/\text{ml}$, ab24590, Abcam, Cambridge, UK), rabbit polyclonal anti-human CD73 antibody (1:100, ab71822, Abcam), rabbit monoclonal anti-human CD90 antibody (1:100, ab92574, Abcam), and rabbit polyclonal anti-human CD105 antibody (1:100, sc-20632, Santa Cruz Biotechnology, Inc., Santa Cruz, CA, USA). Immunofluorescence staining was performed using the secondary antibodies DyLight 549-labeled anti-rabbit IgG (H+L) (KPL, Gaithersburg, MD, USA), DyLight 488-labeled anti-mouse IgG (KPL), and DyLight 549-labeled anti-chicken IgG (H+L) (KPL), which were diluted 1:1000 in 2% BSA for 1 hour at room temperature. Nuclear staining was performed with 2 $\mu\text{g}/\text{ml}$ Hoechst H333342 (Sigma-Aldrich) solution for 2 minutes.

Cell cultures

The lipoaspirate from the HDL was washed with PBS and digested using a solution of 0.075% collagenase from *Clostridium histolyticum* type II (Sigma-Aldrich, St. Louis, MO, USA) in Hank's balanced salt solution (HBSS, Lonza Srl, Milano, Italy) for 3 h at room temperature under slow agitation. At the end of the digestion, the collagenase activity was blocked with an equal volume of complete (cDMEM), which consisted of Dulbecco's modified Eagle's medium (DMEM, Lonza, Italy) supplemented with 10% fetal bovine serum (FBS, Bidachem SpA, Milano, Italy) and 1% penicillin/streptomycin (P/S, EuroClone). After centrifugation for 4 min at 1200 rpm, the pellet was washed in PBS and filtered using a 70- μm cell strainer (BD Biosciences, Mississauga,

Table 1. List of genes analyzed by real-time PCR.

Gene symbol	Description
ABCB1	ATP-binding cassette, sub-family B member 1
ALCAM	Activated leukocyte cell adhesion molecule
ANPEP	Alanyl (membrane) aminopeptidase
ANXA5	Annexin A5
BDNF	Brain-derived neurotrophic factor
BGLAP	Bone gamma-carboxyglutamate (gla) protein
BMP2	Bone morphogenetic protein 2
BMP4	Bone morphogenetic protein 4
BMP6	Bone morphogenetic protein 6
BMP7	Bone morphogenetic protein 7
CASP3	Caspase 3, apoptosis-related cysteine peptidase
CD44	Cluster of differentiation 44 molecule
COL1A1	Collagen, type I, alpha 1
CSF2	Colony stimulating factor 2
CSF3	Colony stimulating factor 3
CTNNB1	Catenin (cadherin-associated protein), beta 1
EGF	Epidermal growth factor
ENG	Endoglin (CD105)
ERBB2	v-erb-b2 avian erythroblastic leukemia viral oncogene homolog 2
FGF10	Fibroblast growth factor 10
FGF2	Fibroblast growth factor 2
FUT1	Fucosyltransferase 1
FUT4	Fucosyltransferase 4
FZD9	Frizzled family receptor 9
GDF15	Growth differentiation factor 15
GDF5	Growth differentiation factor 5
GDF7	Growth differentiation factor 7
GTF3A	General transcription factor IIIA
HAT1	Histone acetyltransferase 1
HDAC1	Histone deacetylase 1
HGF	Hepatocyte growth factor
HNF1A	HNF1 homeobox A
ICAM1	Intercellular adhesion molecule 1
IFNG	Interferon, gamma
IGF1	Insulin-like growth factor 1
IL10	Interleukin 10
IL1B	Interleukin 1, beta
IL6	Interleukin 6
INS	Insulin
ITGA6	Integrin, alpha 6
ITGAV	Integrin, alpha V
ITGAX	Integrin, alpha X
ITGB1	Integrin, beta 1
KDR	Kinase insert domain receptor
KITLG	KIT ligand
LIF	Leukemia inhibitory factor
MCAM	Melanoma cell adhesion molecule
MITF	Microphthalmia-associated transcription factor
MMP2	Matrix metalloproteinase 2
NES	Nestin

Table 1. Cont.

Gene symbol	Description
NGFR	Nerve growth factor receptor
NTSE	5'-nucleotidase (CD73)
NUDT6	Nudix (nucleoside diphosphate linked moiety X)-type motif 6
KAT2B	K(lysine) acetyltransferase 2B
PDGFRB	Platelet-derived growth factor receptor, beta polypeptide
PIGS	Phosphatidylinositol glycan anchor biosynthesis, class S
POU5F1	POU class 5 homeobox 1
PROM1	Prominin 1
PTK2	PTK2 protein tyrosine kinase 2
PTPRC	Protein tyrosine phosphatase, receptor type, C
RUNX2	Runt-related transcription factor 2
SLC17A5	Solute carrier family 17, member 5
SMAD4	SMAD family member 4
SMURF2	SMAD specific E3 ubiquitin protein ligase 2
SOX2	SRY (sex determining region Y)-box 2
SOX9	SRY (sex determining region Y)-box 9
TBX5	T-box 5
TERT	Telomerase reverse transcriptase
TGFB1	Transforming growth factor, beta 1
TGFB3	Transforming growth factor, beta 3
THY1	Thy-1 cell surface antigen
TNF	Tumor necrosis factor
VCAM1	Vascular cell adhesion molecule 1
VEGFA	Vascular endothelial growth factor A
VIM	Vimentin
VWF	Von Willebrand factor
WNT3A	Wingless-type MMTV integration site family, member 3A
ZFP42	Zinc finger protein 42 homolog

doi:10.1371/journal.pone.0110796.t001

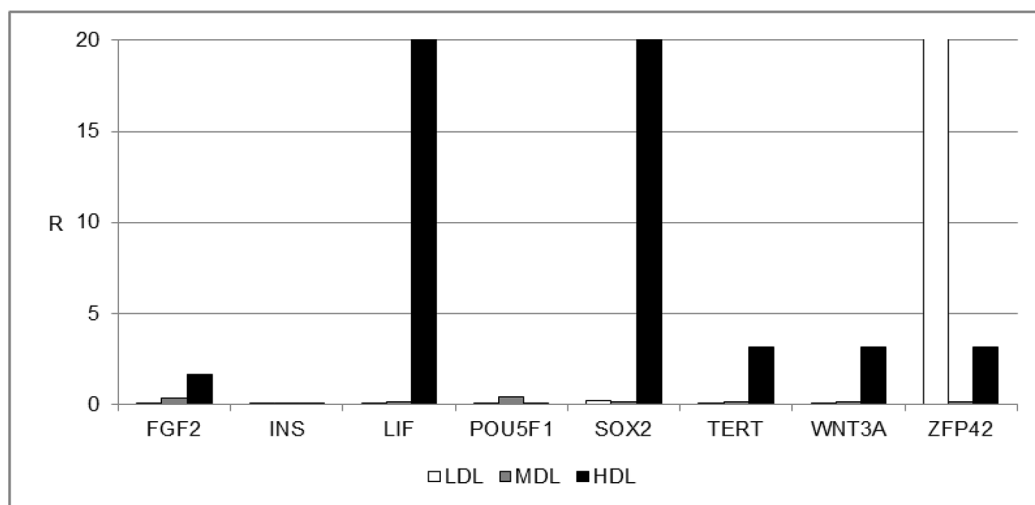


Figure 2. Gene expression profile of stemness markers. Gene expression profile of stemness markers in the LDL (white bars), MDL (grey bars), and HDL (black bars). The results are reported as ratios (R) with respect to the mRNA expression levels of non-centrifuged fat (not shown). doi:10.1371/journal.pone.0110796.g002

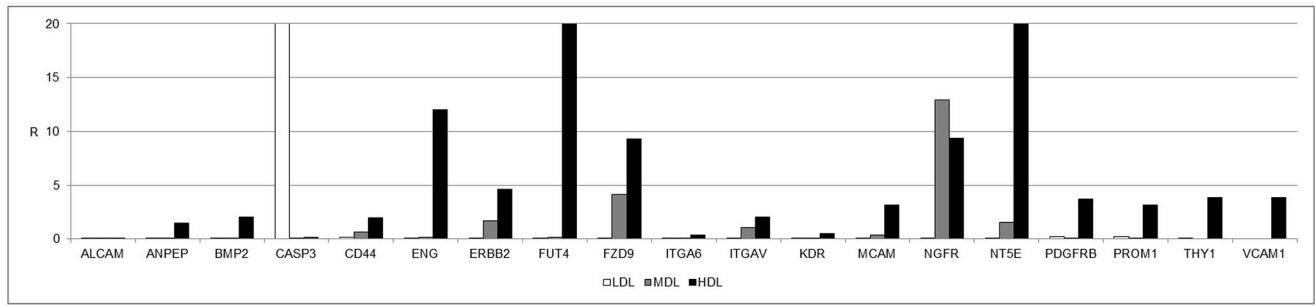


Figure 3. Gene expression profile of mesenchymal stem cell-specific markers. Gene expression profile of mesenchymal stem cell-specific markers in the LDL (white bars), MDL (grey bars), and HDL (black bars). The results are reported as ratios (R) with respect to the mRNA expression levels of non-centrifuged fat (not shown). doi:10.1371/journal.pone.0110796.g003

Ontario, Canada). The cell suspension was resuspended in cDMEM, transferred to a 25-cm² tissue culture flask, and then incubated at 37°C and 5% CO₂.

Subsequently, cells were seeded into seven 35-mm Petri dishes (50,000 cells/dish) and on seven scaffolds (see 3D scaffolds section, 500,000/cm²) and then cultured in seven differentiation media:

- 1) Standard medium (Nonhematopoietic (NH) stem cell medium, Miltenyi Biotec, Bergish Gladbach, Germany);
- 2) Adipogenic differentiation medium (StemMACS AdipoDiff Media, Miltenyi Biotec);
- 3) Endothelial differentiation medium: DMEM containing 10% FBS, 10 ng/ml ECGF (Calbiochem, San Diego, CA, USA), 10 ng/ml bFGF (Prospec, East Brunswick, NJ, USA), 100 ng/ml porcine heparin (Seromed, Berlin, Germany);

- 4) Chondrogenic differentiation medium (StemMACS ChondroDiff Media, Miltenyi Biotec);
- 5) Osteogenic differentiation medium (StemMACS OsteoDiff Media, Miltenyi Biotec);
- 6) Neuronal differentiation medium: NeuroBasal medium (Gibco by Life Technologies, Paisley, UK) containing 1% FBS, 2% B27 (Gibco), NGF (Prospec), 100 ng/ml BDNF (Prospec), and 20 ng/ml NT3 (Prospec);
- 7) Glial differentiation medium: NeuroBasal medium containing 1% FBS, 1% N2 supplement (Gibco), 4 μM forskolin (Merck Millipore, Darmstadt, Germany), and 10 ng/ml heregulin β (Prospec).

The cells were cultured as a monolayer or on 3D scaffolds in standard, endothelial, adipogenic, and chondrogenic media for up

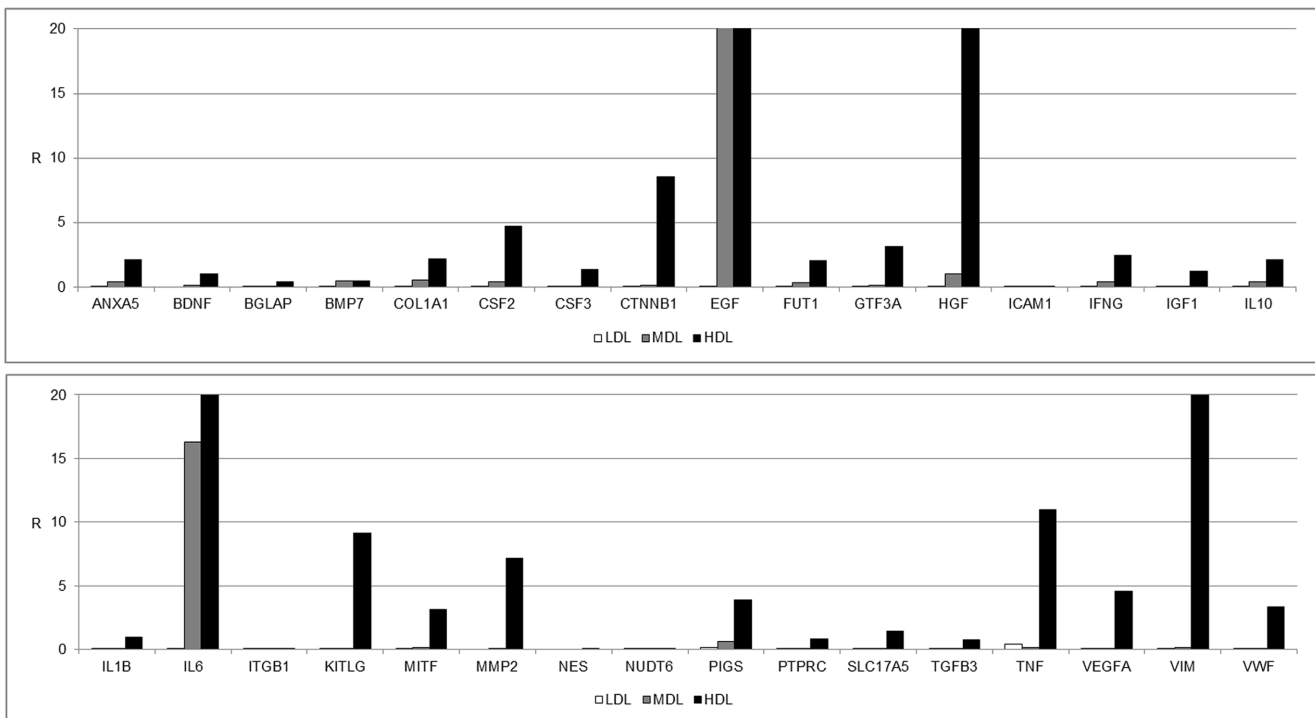


Figure 4. Gene expression profile of genes associated with mesenchymal stem cell markers. Gene expression profile of genes associated with mesenchymal stem cell markers in the LDL (white bars), MDL (grey bars), and HDL (black bars). The results are reported as ratios (R) with respect to the mRNA expression levels of non-centrifuged fat (not shown). doi:10.1371/journal.pone.0110796.g004

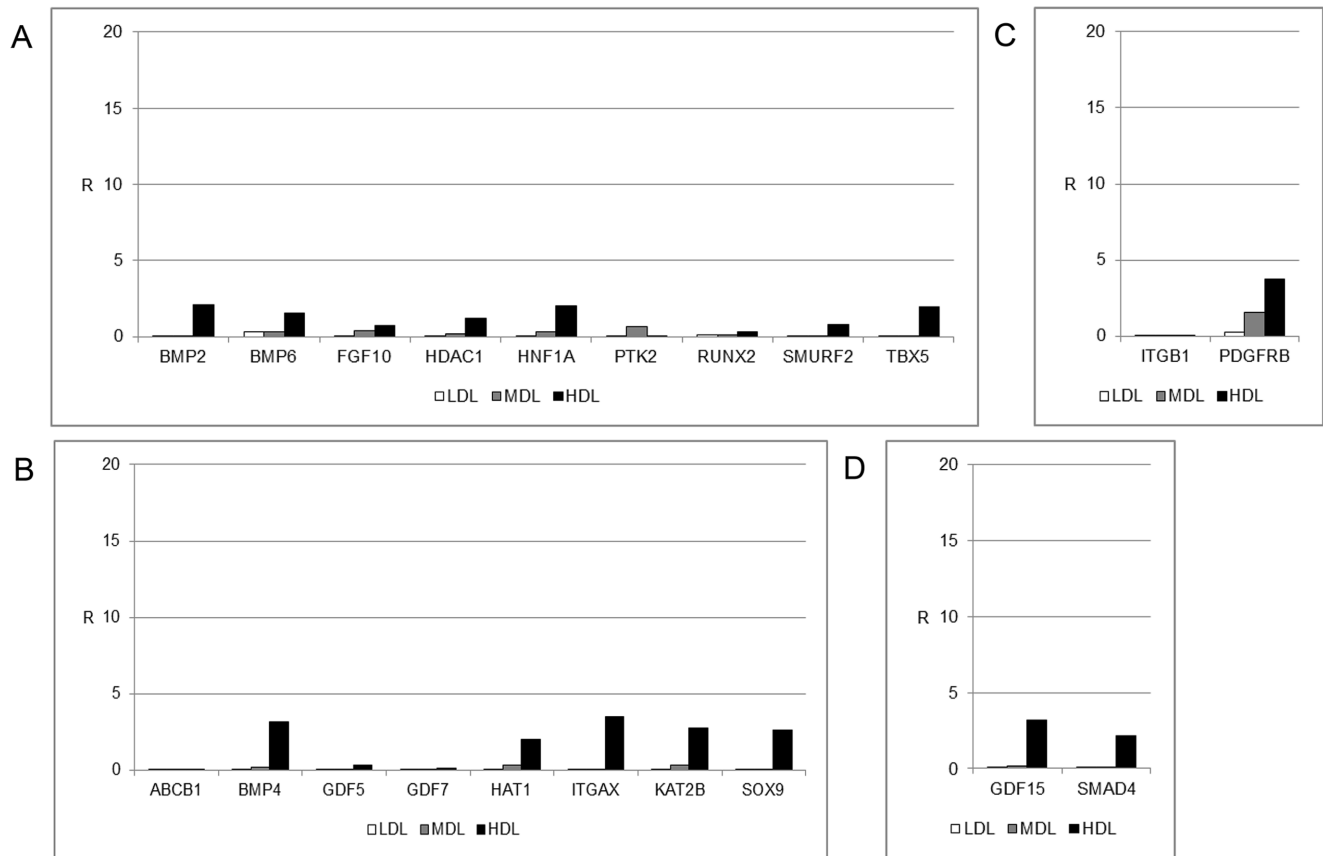


Figure 5. Gene expression profile of genes associated with mesenchymal stem cell markers. Gene expression profile of genes associated with mesenchymal stem cell markers in the LDL (white bars), MDL (grey bars), and HDL (black bars). The results are reported as ratios (R) with respect to the mRNA expression levels of non-centrifuged fat (not shown). (A) Osteogenesis, (B) chondrogenesis, (C) myogenesis, and (D) tenogenesis. doi:10.1371/journal.pone.01110796.g005

to 21 days and in osteogenic, neurogenic and glial media for up to 28 days. The media were changed every 3 days.

3D scaffolds

Scaffold for osteogenic, endothelial, neuronal, and glial commitment: 1×1 cm non-woven meshes made of a linear derivative of hyaluronic acid (HYA) (HYAFF 11, Fidia Advanced Biopolymers, Abano Terme, Padova, Italy).

Scaffold for adipogenic commitment: cylindrical sponges made of HYA (HYAFF 11).

Scaffold for chondrogenic commitment: 1×1 cm bovine-derived pericardium membrane (Chondro-Gide, Geistlich Pharma AG, Wolhusen, Switzerland).

Scanning electron microscopy (SEM)

Samples were fixed with 2.5% glutaraldehyde (glutaraldehyde solution Grade I, 25% in H₂O; G5882, Sigma-Aldrich) in 0.1 M cacodylate (sodium cacodylate trihydrate; C0250, Sigma-Aldrich) buffer for 1 h before critical-point drying, followed by gold-palladium coating. All micrographs were obtained using a JEOL 6360LV SEM microscope (JEOL, Tokyo, Japan). The SEM analysis was performed at the Interdepartmental Service Center (CUGAS, University of Padova, Padova, Italy).

Statistical analysis

One-way analysis of variance (ANOVA) was used for the data analyses. A repeated-measures ANOVA with a post-hoc analysis

using Bonferroni's correction for multiple comparisons was performed, and t-tests were used to determine significant differences ($p < 0.05$). Repeatability was calculated as the standard deviation of the difference between measurements. All testing was performed using the SPSS 16.0 software (SPSS Inc., Chicago, IL, USA) (licensed by the University of Padova).

Results

Using Coleman's procedure, the abdominal fat of healthy patients was aspirated and centrifuged, thus producing three layers: an upper yellow layer of oil, a middle layer of adipose tissue, and a bottom layer of blood. The top and bottom layers were discarded. The middle layer was divided into three distinct parts: a low-density layer (LDL), a middle-density layer (MDL), and a high-density layer (HDL) (Figure 1A). The cell quantity of each layer was determined by measuring the DNA content (Figure 1B). The quantity of cells was similar for each subsequently analyzed layer.

Molecular, morphological and cellular analyses were performed on these layers.

To characterize the stemness properties of the cells within the fat, the mRNA from each layer was extracted and analyzed by real-time PCR. The analyzed genes are listed in Table 1. Figure 2 shows the gene expression of stemness markers in the LDL, MDL, and HDL. Non-centrifuged fat was used as a control. Significant mRNA expression was detected for LIF, SOX2, TERT, WNT3A, and ZFP42. The HDL exhibited higher levels of LIF and SOX2

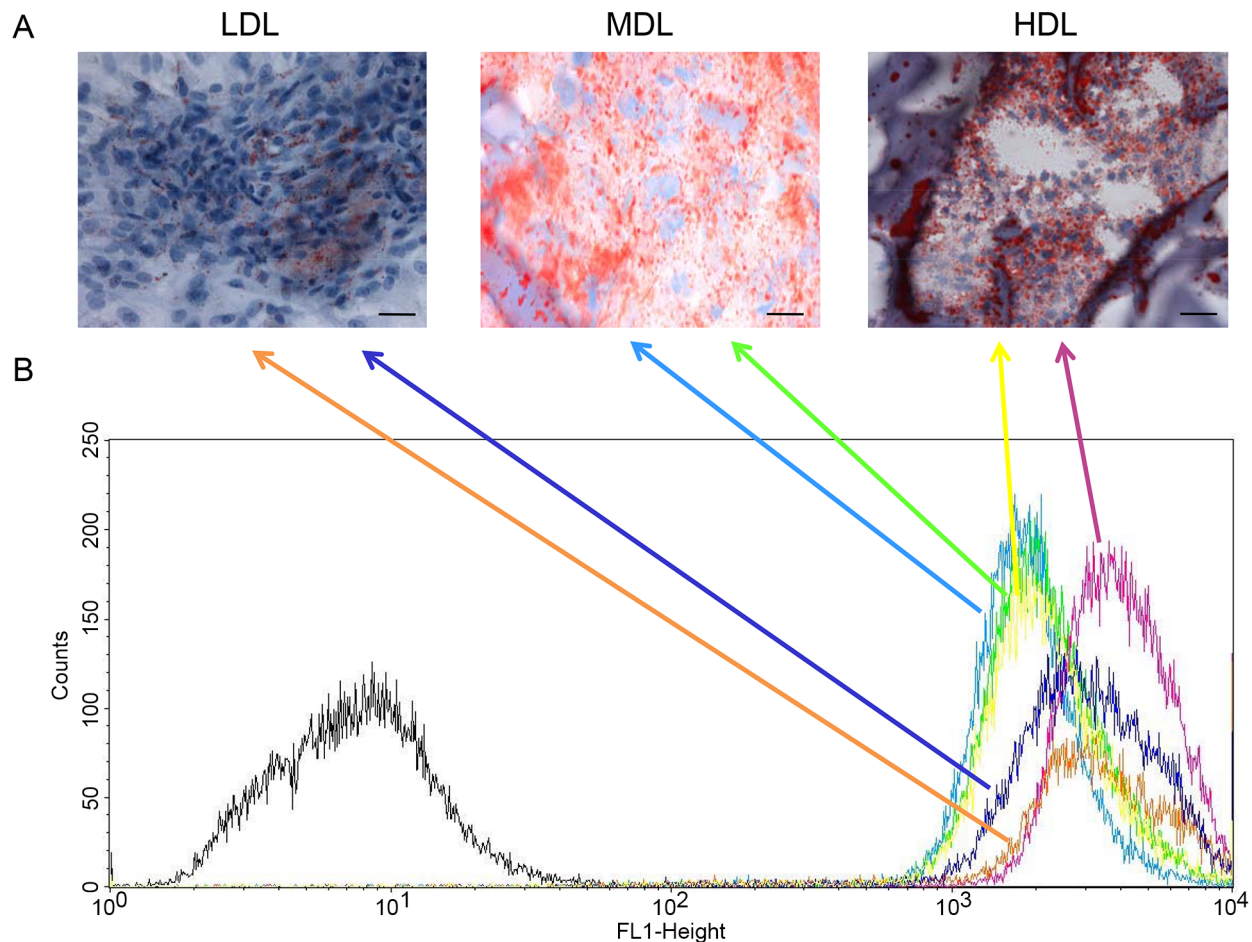


Figure 6. Evaluation of the lipid contents of the LDL, MDL, and HDL. (A) ORO staining (red drops in each panel) shows higher lipid contents in the MDL and in the HDL compared with that of the LDL (scale bar = 100 μ m). (B) Semi-quantitative analysis of the lipid contents. The signals from the LDL are in blue and orange, signals from the MDL are in sky blue and green, and signals from the HDL are in yellow and purple. doi:10.1371/journal.pone.01110796.g006

gene expression compared with those expression levels in the MDL and in the LDL, whereas the LDL displayed higher expression of the ZFP42 gene, which is a marker of pluripotent stem cells [28].

The characteristics of cells from the different layers were analyzed in greater detail. Figure 3 shows the expression of important markers for several cell processes, such as vascularization, which is mediated by stem cells (ENG) and by mesenchymal stem cells (CD44, FZD9, and NT5E), and migration and functional properties related to stemness, such as FUT4. The expression levels of all these markers were higher in the HDL than in the MDL or the LDL.

Finally, we focused our attention on the expression of specific mesenchymal stem markers, as shown in Figure 4. Several genes were expressed, including ANXA5, COL1A1, CTNNB1, EGF, FUT1, HGF, KITLG, MITF, MMP2, and VIM. High levels of vascular-inducing factors, such as VEGFA and VWF, have also been detected. No markers for commitment into osteogenic, chondrogenic, myogenic, or tenogenic lineages were present in the three layers after centrifugation (Figure 5).

Furthermore, we analyzed the adipogenic properties of each layer by measuring the lipid content. As shown in Figure 6A, each layer of fat displayed cells able to store lipids in their cytoplasm. Indeed, the cells from each layer were positively stained with

ORO; however, higher quantities of lipid-containing cells were present in the MDL and in the HDL. Similar findings were obtained when we performed a semi-quantitative analysis (Figure 6B) of the staining inside the cytoplasm of cells from the different layers. The cells from the LDL stored less lipids than the cells from the bottom level.

We analyzed the presence of the specific stem cell markers CD73 (NT5E), CD90, and CD105 (ENG) using immunofluorescence. As shown in Figure 7, the positive cells for these markers were found in all layers. However, a greater number of positive cells was found in the HDL than in the LDL.

The commitment ability of the stem cells present in the HDL was analyzed using *in vitro* experiments. Cells derived from the bottom level were seeded both as monolayers (2D culture) and on three-dimensional scaffolds (3D cultures) and cultured for up to 28 days in the presence of specific differentiation media (Figure 8). The commitment into osteogenic, adipogenic, chondrogenic, neuronal, glial, and endothelial lineages was detected using immunofluorescence and gene expression analyses. For the osteogenic commitment, the cells in monolayers and on non-woven HYA-based scaffolds were treated with an osteogenic inducer. As reported in Figure 8A, osteonectin expression was evaluated using immunofluorescence in both 2D and 3D cultures. Gene expression of 3D cultures was also used to better

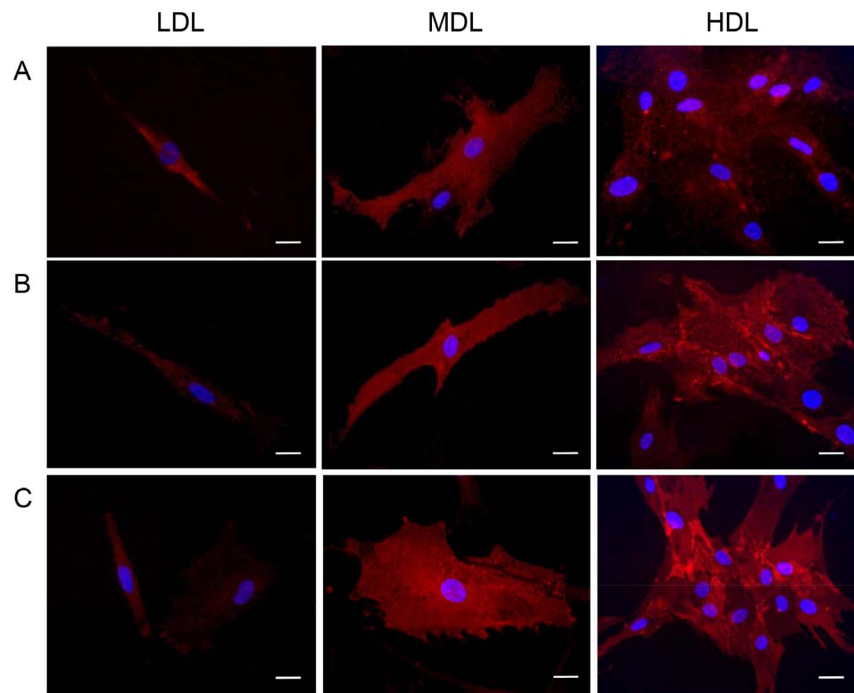


Figure 7. Immunostaining of stem cell markers present in the LDL, MDL, and HDL. Positive (red) cells for (A) CD73, (B) CD90, and (C) CD105 (scale bar = 10 μ m).
doi:10.1371/journal.pone.0110796.g007

characterize this commitment. As reported in Figure 8A, genes for osteogenic commitment, such as osteopontin (OPN), osteonectin (ON), osteocalcin (OCN), and type I collagen (COL1A1), were expressed, whereas genes related to other lineages were not expressed. The results related to the adipogenic commitment are reported in Figure 8B. Morphological analyses performed with ORO staining of lipid drops indicated many positively stained cells. This result was also confirmed by SEM analyses of the 3D cultures (cells seeded onto HYA-based sponges), in which the typical adipogenic round shape was evident. Genes related to the adipogenic phenotype, such as peroxisome proliferator-activated receptor gamma (PPARG), lipoprotein lipase (LPL), solute carrier family 2 (facilitated glucose transporter), member 4 (GLUT4), and adiponectin (ADIPOQ), but not those genes related to other lineages, were expressed. For chondrogenic commitment, only 3D cultures were prepared because of the characteristics of this tissue. In this case, cells derived from the HDL were seeded onto a bovine-derived pericardial membrane and cultured with chondrogenic medium. After 28 days, the cells organized themselves into typical clusters and expressed only type II collagen (COL2A1) but no other markers (Figure 8C). Neuronal and glial commitment analyses were also performed on 3D HYA-based scaffolds, which were non-woven meshes. As reported in Figure 8D (for the neuronal commitment) and in Figure 8E (for the glial commitment), the cells expressed the neuronal marker beta III tubulin (TUBB3) and the glial marker glial fibrillary acidic protein (GFAP) at both protein and mRNA levels.

The endothelial properties of the stem cells present in the HDL were also analyzed (Figure 8F). Commitment was evaluated using positive endothelial markers, such as von Willebrand factor (VWF) and CD31, in both 2D and 3D cultures (on HYA non-woven meshes). In the 3D scaffolds, the cells organized into micro-capillary vessels. The gene expression of endothelial markers, such

as CD31, VWF, and vascular endothelial growth factor (VEGF), was also present, without the expression of other cell markers.

Discussion and Conclusions

Fat grafting has become popular as a stand-alone technique or as a part of a combined procedure for facial rejuvenation and for reconstructive craniofacial surgery [1]. Autologous tissue is completely biocompatible and is typically the safest choice for altering facial volume or contours. Fat grafts can be placed in such a manner that these grafts are long-lasting, completely integrated, and natural looking. The transfer technique is also known as structural fat grafting (SFG), or lipostructure, and requires the centrifugation of fat and its implantation into a specific site to be restored [29,30]. Currently, no attention has been given to the stemness properties of the cells that are injected into the patient. In this study, we performed molecular analyses of the stemness properties of cells distributed in the fat following the centrifugation required by Coleman's procedure.

The distribution of stem cells across the three detected layers has been well defined. In the LDL, a few (but important) stem cell markers, such as ZFP42, were expressed (Figure 2). This finding indicates the presence of small multipotent stem cells in this layer (dimensions of 20–50 nm, data not shown). The MDL did not express stemness markers other than EGF. The stromal component was predominantly represented in the HDL, where high expression levels of mesenchymal stem cell markers (LIF, SOX2, WNT3A, CTNBN1, FUT4, EGF, KITLG, HGF, and VIM) were detected (Figure 3). Another notable finding is the high expression levels of endothelial markers (such as VEGFA) in this layer, indicating the high vasculogenic properties of the cells in this layer (dimension of the cells in this layer ranged from 50–100 nm, data not shown) (Figure 4). No specific markers for commitment into osteogenic, chondrogenic, myogenic, or tenogenic lineages have

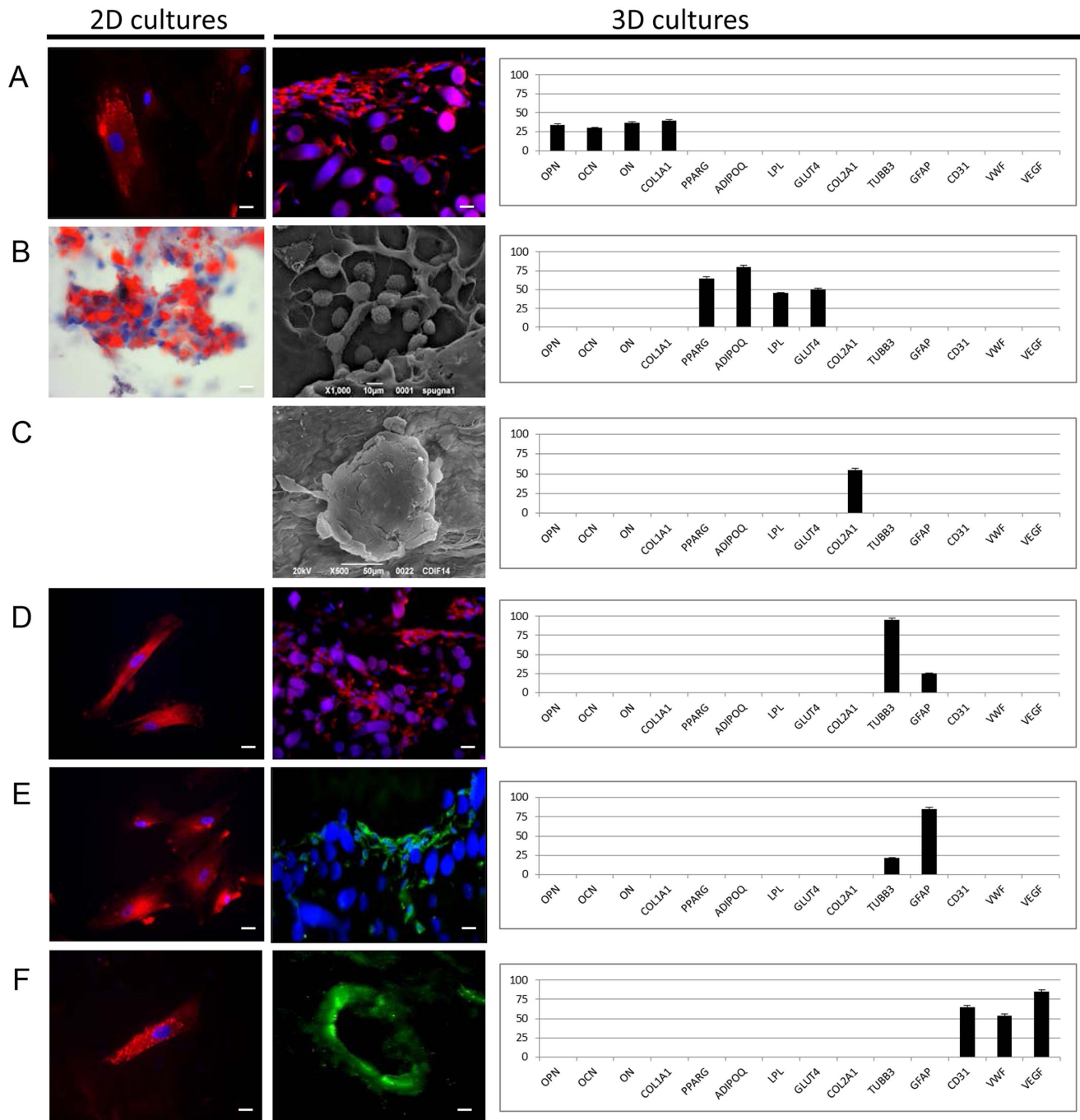


Figure 8. Commitment ability of stem cells present in the HDL. (A) Osteogenic commitment. Immunofluorescence confirms positive staining for osteonectin (red) in both 2D cultures (scale bar = 20 μ m) and 3D cultures (scale bar = 50 μ m). Real-time PCR detects the expression of osteopontin (OPN), osteonectin (ON), osteocalcin (OCN), and type I collagen (COL1A1), which are typical markers of osteogenic commitment. (B) Adipogenic commitment. ORO staining confirms lipid deposition inside the cytoplasm (red) in 2D cultures (scale bar = 50 μ m). SEM analysis of 3D cultures reveals the typical adipogenic round shape of cells (scale bar = 10 μ m). Genes related to the adipogenic phenotype, such as PPARG, LPL, GLUT4, and ADIPOQ, are expressed. (C) Chondrogenic commitment. In the 3D cultures, the cells are organized into their typical clusters, as shown by SEM analysis (scale bar = 50 μ m), and only express type II collagen (COL2A1), as detected by real-time PCR. (D) Neuronal commitment. Immunofluorescence confirms positive staining for TUBB3 (red) in both 2D cultures (scale bar = 40 μ m) and 3D cultures (scale bar = 100 μ m). High expression of TUBB3 and low expression of GFAP are evident. (E) Glial commitment. Immunofluorescence confirms positive staining for GFAP (red, scale bar = 20 μ m) and 3D cultures (green, scale bar = 100 μ m), where significant GFAP mRNA expression is also detectable. (F) Endothelial commitment. Immunofluorescence confirms positive staining for VWF (red) in 2D cultures (scale bar = 20 μ m) and for CD31 (green) in 3D cultures (scale bar = 100 μ m). In the 3D scaffolds, the cells are also able to organize into micro-capillary vessels. Gene expression of endothelial markers, such as CD31 and VEGF, is clearly detectable. doi:10.1371/journal.pone.0110796.g008

been detected (Figure 5); however, this absence is most likely the result of a lack of commitment conditions, such as specific medium, growth factors, or an appropriate scaffold. The expression of some inflammatory cytokines, such as IL1B and TNF, and of apoptotic molecules, including CASP3, has also been detected. Thus, the mechanical procedure of lipoaspiration may act as an inflammatory stimulus in the adipose tissue.

To better characterize the cell populations of each layer, we also analyzed the adipogenic properties of each layer by measuring the lipid contents (Figure 6) and by immunofluorescence analyses of cell-surface stem cell markers (Figure 7).

As shown in Figure 6, each layer contained cells able to store lipids in their cytoplasm, confirming the presence of mature adipocytes. We also analyzed the expression of the stem cell markers CD73, CD90, and CD105. As reported in Figure 7, we observed expression of these markers in all three layers; however, a greater number of positive cells were detected in the HDL than in the LDL.

Finally, the commitment ability of the stem cells present in the HDL was analyzed using *in vitro* experiments. Our results confirmed that, in presence of specific growth factors, cells

differentiated into several lineages, including osteogenic, adipogenic, chondrogenic, neuronal, glial, and endothelial lineages (Figure 8). The obtained results confirm that the distribution of stem cells into the three layers is well defined. This information is useful for surgeons who may apply the different layers in different situations. We speculate that the HDL contains a larger quantity of stem cells and a larger vascular potential compared with the other fractions; thus, this layer could be used for the regeneration of large defects. The medium layer, which has a larger quantity of differentiated cells, could be useful for increasing volume, and the layers enriched with multipotent cells are suitable for all uses.

In conclusion, we hypothesize that centrifugation creates a graded density of fat with varying characteristics that influence lipoaspirate persistence, properties, and quality.

Author Contributions

Conceived and designed the experiments: BZ LC. Performed the experiments: LF CG RT GE. Analyzed the data: MG PP EB. Contributed reagents/materials/analysis tools: BZ. Wrote the paper: AP BZ.

References

- Coleman SR (1997) Facial recontouring with lipostructure. *Clin Plast Surg* 24: 347–367.
- Coleman SR (2001) Structural fat grafts: the ideal filler? *Clin Plast Surg* 28: 111–119.
- Coleman SR (2004) Structural fat grafting. St Louis, MO: Quality Medical Publishing, Inc.
- Fraser JK, Wulur I, Alfonso Z, Hedrick MH (2006) Fat tissue: an underappreciated source of stem cells for biotechnology. *Trends Biotechnol* 24: 150–154.
- Rigotti G, Marchi A, Sbarbati A (2009) Adipose-derived mesenchymal stem cells: past, present, and future. *Aesthetic Plast Surg* 33: 271–273.
- Strem BM, Hicok KC, Zhu M, Wulur I, Alfonso Z, et al. (2005) Multipotential differentiation of adipose tissue-derived stem cells. *Keio J Med* 54: 132–141.
- Bucky LP, Kanchwala SK (2007) The role of autologous fat and alternative fillers in the aging face. *Plast Reconstr Surg* 120: 89S–97S.
- Clauser L, Sarti E, Dalleria V, Galiè M (2004) Integrated reconstructive strategies for treating the anophthalmic orbit. *J Craniomaxillofac Surg* 32: 279–290.
- Clauser LC, Tieghi R, Galiè M (2011) Structural fat grafting: facial volumetric restoration in complex reconstructive surgery. *J Craniofac Surg* 22: 1695–1701.
- Moseley TA, Zhu M, Hedrick MH (2006) Adipose-derived stem and progenitor cells as fillers in plastic and reconstructive surgery. *Plast Reconstr Surg* 118: 121S–128S.
- Clauser L, Polito J, Mandrioli S, Tieghi R, Denes SA, et al. (2008) Structural fat grafting in complex reconstructive surgery. *J Craniofac Surg* 19: 187–191.
- Clauser L (2009) Optimizing maxillofacial and craniofacial results. In: Coleman SR, Mazzola RF, editors. *Fat injection from filling to regeneration*. St Louis, MO: Quality Medical Publishing, Inc. pp. 475–500.
- Clauser L (2009) Optimizing maxillofacial and craniofacial results. Presented at: American Society of Plastic Surgeons Annual Meeting, Seattle, WA.
- Clauser LC, Tieghi R, Consorti G (2010) Parry-Romberg syndrome: volumetric regeneration by structural fat grafting technique. *J Craniomaxillofac Surg* 38: 605–609.
- Consorti G, Tieghi R, Clauser LC (2012) Frontal linear scleroderma: long-term result in volumetric restoration of the fronto-orbital area by structural fat grafting. *J Craniofac Surg* 23: e263–265.
- Coleman SR, Saboero A, Sengelmann R (2009) A comparison of lipoatrophy and aging: volume deficits in the face. *Aesthetic Plast Surg* 33: 14–21.
- Giugliano C, Benitez S, Wisnia P, Sorolla JP, Acosta S, et al. (2009) Liposuction and lipoinjection treatment for congenital and acquired lipodystrophies in children. *Plast Reconstr Surg* 124: 134–143.
- Mojallal A, Foyatier JL, Voulliamume D, Comparin JP (2004) Clinical evaluation of structural fat tissue graft (Lipostructure) in volumetric facial restoration with face-lift. About 100 cases. *Ann Cir Plast Esthet* 49: 437–455.
- Kawamoto HK (2009) Fat injection and craniofacial surgery. In: Coleman SR, Mazzola RF, editors. *Fat injection from filling to regeneration*. St Louis, MO: Quality Medical Publishing, Inc. pp. 447–474.
- Mojallal A, Auxenfans C, Lequeux C, Braye F, Damour O (2008) Influence of negative pressure when harvesting adipose tissue on cell yield of the stromal-vascular fraction. *Biomed Mater Eng* 18: 193–197.
- Mojallal A, Foyatier JL (2004) The effect of different factors on the survival of transplanted adipocytes. *Ann Chir Plast Esthet* 49: 426–436.
- Mojallal A, Shipkov C, Braye F, Breton P, Foyatier JL (2009) Influence of the recipient site on the outcomes of fat grafting in facial reconstructive surgery. *Plast Reconstr Surg* 124: 471–483.
- Pu LL, Coleman SR, Cui X, Ferguson RE Jr, Vasconez HC (2008) Autologous fat grafts harvested and refined by the Coleman technique: a comparative study. *Plast Reconstr Surg* 122: 932–937.
- Coleman SR (1995) Long-term survival of fat transplants: controlled demonstrations. *Aesthetic Plast Surg* 19: 421–425.
- Fagrell D, Eneström S, Berggren A, Kniola B (1996) Fat cylinder transplantation: An experimental comparative study of three different kinds of fat transplantation. *Plast Reconstr Surg* 98: 90–96.
- Kokai LE, Rubin JP, Marra KG (2005) The potential of adipose derived adult stem cells as a source of neuronal progenitor cells. *Plast Reconstr Surg* 116: 1453–1460.
- Rigotti G, Marchi A, Galiè M, Baroni G, Benati D, et al. (2007) Clinical treatment of radiotherapy tissue damage by lipoaspirate transplant: a healing process mediated by adipose-derived adult stem cells. *Plast Reconstr Surg* 119: 1409–1422.
- Guallar D, Pérez-Palacios R, Climent M, Martínez-Abadía I, Larraga A, et al. (2012) Expression of endogenous retroviruses is negatively regulated by the pluripotency marker Rex1/Zfp42. *Nucleic Acids Res* 40: 8993–9007.
- Livaoglu M, Yavuz E (2009) Soft tissue augmentation with autologous fat graft: the dissected pouch technique. *J Cutan Aesthet Surg* 2: 21–25.
- Perrot P, Rousseau J, Bouffaut AL, Rédini F, Cassagnau E, et al. (2010) Safety concern between autologous fat graft, mesenchymal stem cell and osteosarcoma recurrence. *PLoS One* 5: e10999.